minerals

MDPI

Article

Influence of Microbubble on Fine Wolframite Flotation

Penggang Wei [1], Liuyi Ren [1,2,*], Yimin Zhang [1,2,3,4] and Shenxu Bao [1,2]

[1] School of Resources and Environmental Engineering, Wuhan University of Technology, Wuhan 430070, China; wpg0310@163.com (P.W.); zym126135@126.com (Y.Z.); sxbao@whut.edu.cn (S.B.)
[2] Hubei Key Laboratory of Mineral Resources Processing and Environment, Wuhan University of Technology, Wuhan 430070, China
[3] State Environmental Protection Key Laboratory of Mineral Metallurgical Resources Utilization and Pollution Control, Wuhan University of Science and Technology, Wuhan 430081, China
[4] Hubei Collaborative Innovation Center for High Efficient Utilization of Vanadium Resources, Wuhan University of Science and Technology, Wuhan 430081, China
* Correspondence: rly1015@163.com

Abstract: The recovery of fine wolframite is low when using traditional flotation that does not use a microbubble. In this study, a microbubble was introduced into the fine wolframite flotation system; −20 μm wolframite was used as an experiment sample and octyl hydroxamic acid as the collector. The recovery of microbubble flotation reached 84.07%, which is about 12.04% higher than that of traditional flotation. A single-factor flotation experiment, high-speed camera analysis, and SEM (Scanning Electron Microscopy) analysis were used to study the influence of microbubbles on the flotation of fine wolframite. The results show that fine wolframite will more easily agglomerate under the action of microbubbles. The octyl hydroxamic acid adsorbed on the surface of wolframite treated with microbubbles is denser and more abundant.

Keywords: wolframite; fine particles; microbubble; flotation

Citation: Wei, P.; Ren, L.; Zhang, Y.; Bao, S. Influence of Microbubble on Fine Wolframite Flotation. *Minerals* **2021**, *11*, 1079. https://doi.org/10.3390/min11101079

Academic Editor: Luis A. Cisternas

Received: 2 September 2021
Accepted: 27 September 2021
Published: 30 September 2021

1. Introduction

In view of the coarse disseminated particle size, large specific gravity, and relatively simple composition of wolframite, the main process of separation is gravity separation [1]. In the process of gravity separation, due to the brittle nature of tungsten ore, it is easy to over-grind and produce fine mud; most of the fine mud is embedded with a finer grain size, and there are many useful metal minerals associated with it. Approximately 20% of tungsten is lost in fine mud every year in the world [2]. Therefore, the research of fine-grained mineral recovery technology is of great significance to the recovery and utilization of wolframite. Compared with coarse-grained minerals, fine-grained minerals have different chemical and hydrodynamic conditions and a larger surface area, which means that they have a lower probability of collision with bubbles [3].

Flotation is a commonly used separation method for fine-grain wolframite. Wolframite flotation has a high recovery performance for particle sizes of 10–100 μm, while the flotation efficiency of particles below this range drops sharply [4]. Since the middle particles as carriers are reduced, the collision and adhesion between the fine particles and the bubbles are decreased, making it difficult for the fine particles to float [5]. The main mechanism of collision is interception [6], and a fine particle size will lead to low collision efficiency, which is not conducive to the contact between mineral particles and air bubbles. Mechanical effects also affect the collision process, such as stirring. Stirring provides energy input for the flotation process, which promotes the collision of bubbles and particles [7]. The wrap angle between bubbles and particles is an intuitive manifestation of attachment and detachment. As the reaction time increases, more and more particles are attached to the surface of the bubbles [8].

Similarly an important parameter that affects the probability of collision is the bubble radius [9]. The reason for the low collision probability of ultrafine particles is mainly due to

their small mass, but it can be improved to a certain extent by finer bubbles [10,11]. After theoretical and experimental research, Ready and Ratcliff proposed the collision probability formula to prove that reducing the bubble size can significantly increase the collision probability [12,13]. Safari also developed an attachment–detachment kinetic model that proves the relationship between particle and bubble size and flotation efficiency [14,15]. Consequently, micro-nanobubbles are an important direction used to solve the flotation of fine wolframite. The diameter of nanobubbles is only less than 1 μm, which is characterized by inherent high additional force, and, due to its small size, the ascent speed and the speed of rebounding from the particle surface are very small, therefore, it has a smaller separation distance [12,16].

At present, scholars have introduced microbubbles into the field of non-metallic minerals, such as quartz. By adding microbubbles, Farrokhpay et al. [17] reduced the amount of collector used in flotation quartz and increased the recovery rate. Bu et al. [18] increased the recovery of clean coal from 53.94% to 62.78% with the cyclonic microbubble flotation column technology. Santana et al. [19] confirmed that compared with traditional flotation, microbubble flotation can effectively improve the flotation recovery and ore grade of fine apatite. In the field of metal mining, Rahman et al. [20] designed a nano-microbubble generator independently, which was used to increase the recovery of chalcopyrite fine and ultrafine particles to between 16% and 21%. In the process of separating zinc oxide particles from the mixture of zinc oxide and silica powder, Parmar et al. [21] used ionic microbubbles to improve the selectivity of the flotation system. Many scholars above used experiments to prove the feasibility of microbubble flotation in solving the problem of the difficult selection of fine-grained minerals. This paper intends to use microbubble flotation instead of traditional flotation to improve the flotation recovery rate of fine wolframite.

2. Materials and Methods

2.1. Materials

The wolframite sample was from the Mahuaping Tungsten Mine in Hutiaoxia, Shangri-La, Yunnan. The purity WO_3 was 97%. The X-ray diffraction analysis of the obtained wolframite is shown in Figure 1.

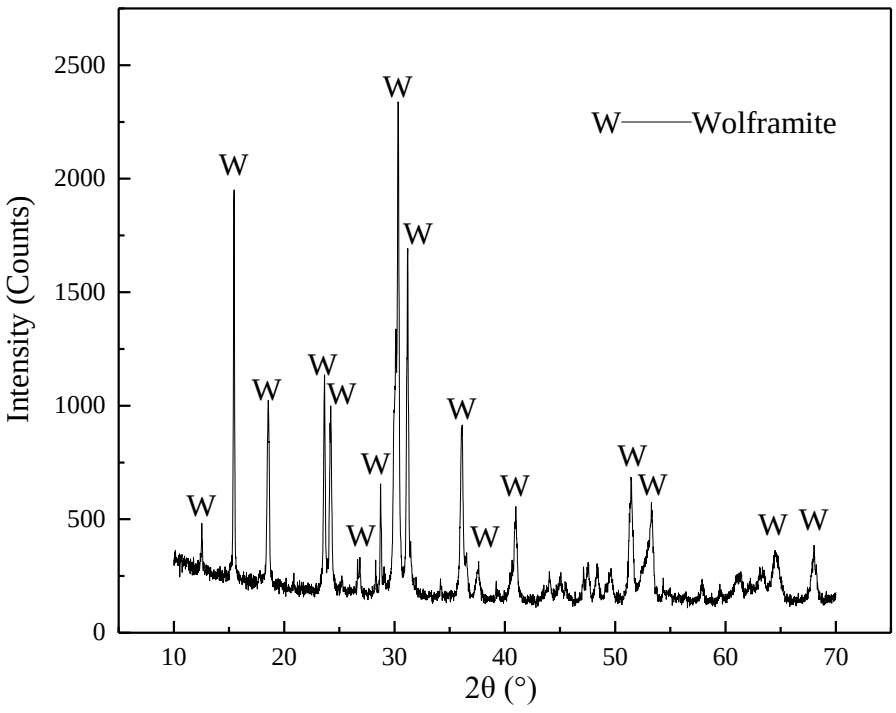

Figure 1. XRD diffraction pattern of wolframite single mineral.

It can be seen from Figure 1 that larger crystal grains and better crystallinity was found in the wolframite sample, and the test requirements are met because of this pure mineral.

Wolframite samples were prioritized for pretreatment. The ore samples were put into a planetary ball mill and ground several times until it was below 38 μm. Then, a large graduated cylinder was used to hydraulically settle the −38 μm particle size sample, then the −20 μm wolframite was obtained. In the test, the slurry concentration was 2%. The particle size analysis of the obtained wolframite is shown in Figure 2 with the particle size of the prepared wolframite samples −20 μm, and D_{90} = 11.35 μm, which meets the test requirements.

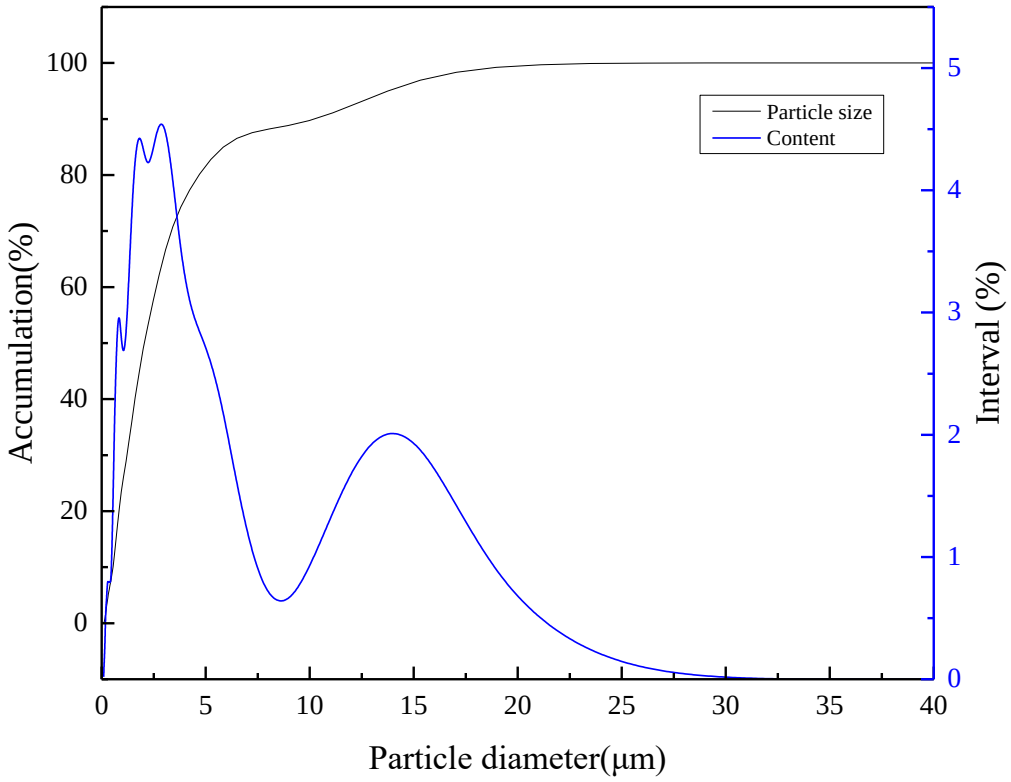

Figure 2. Particle size analysis of wolframite single mineral.

The purity of the reagent octyl hydroxamic acid (Aladdin Biochemical Technology Co., Ltd) used in the experiment exceeds 98%. Lead nitrate is a standard solution of 0.1 mol/L. Hydrochloric acid and sodium hydroxide are analytical grade. A 1.0% dilute hydrochloric acid solution and 4% sodium hydroxide solution with a mass concentration of 1.0% were prepared.

2.2. Single Mineral Flotation

The above-mentioned wolframite pure mineral was regarded as the flotation raw ore. Flotation was carried out in a 30 mL XFGC hanging tank flotation machine (Type II, Jilin Exploration Machinery Plant, Jilin, China)with a spindle speed of 1992 r/min. An amount of 2 g wolframite was used for each test. First, an appropriate amount of deionized water was added to the flotation tank. The proper pH value was adjusted with 1.0% dilute hydrochloric acid solution and 4% sodium hydroxide solution for 2 min. The slurry was stirred for 2 min with collectors one by one. Flotation was carried out for 5 min. The entire flotation process was manual foam scraping. The foam product was filtered, dried, weighed, and the recovery was calculated. The microbubble flotation was carried out by pretreating minerals with microbubbles. The ultra-micron bubble generating device produced by Xiazhichun Company (Yunnan, China) was used to generate microbubbles.

The particle size of the bubbles that can be generated is between 4 μm and 200 nm, and the gas holdup rate is 90%. The ultrasonic cavitation in the instrument is the cause of microbubbles [22]. The micro-nanobubbles are rich in the milky white solution produced by the generator. The large bubbles in the solution will quickly burst and dissipate, and the final solution will turn from milky white to colorless. The solution is ready to use, and should not be stored.

2.3. Zeta Potential Analysis

The test used Malvern ZEN3690 Zeta Potential Analyzer (Malvern Panalytical, Malvern, UK). The ore sample was ground to 2 μm through an agate mortar. In total, 30 mg mineral samples were weighed each time and placed in a 100 mL beaker, 40 mL deionized water was added, and the pH was adjusted with the solution. The addition of reagents was consistent with the conditions of flotation. After stirring for 10 min with a magnetic stirrer, the dynamic potential of the mineral surface was measured. Each sample was measured 3 times and the average value was taken.

2.4. High-Speed Camera Analysis

A Mega Speed MS130K high-speed camera (Mega Speed, Minnedosa, MB, Canada) was used here to study bubble property and the interaction between wolframite particles and bubbles. The maximum resolution of the camera can reach 1920 × 1080. The shutter speed is 2 μs. The high-speed camera system is shown in Figure 3.

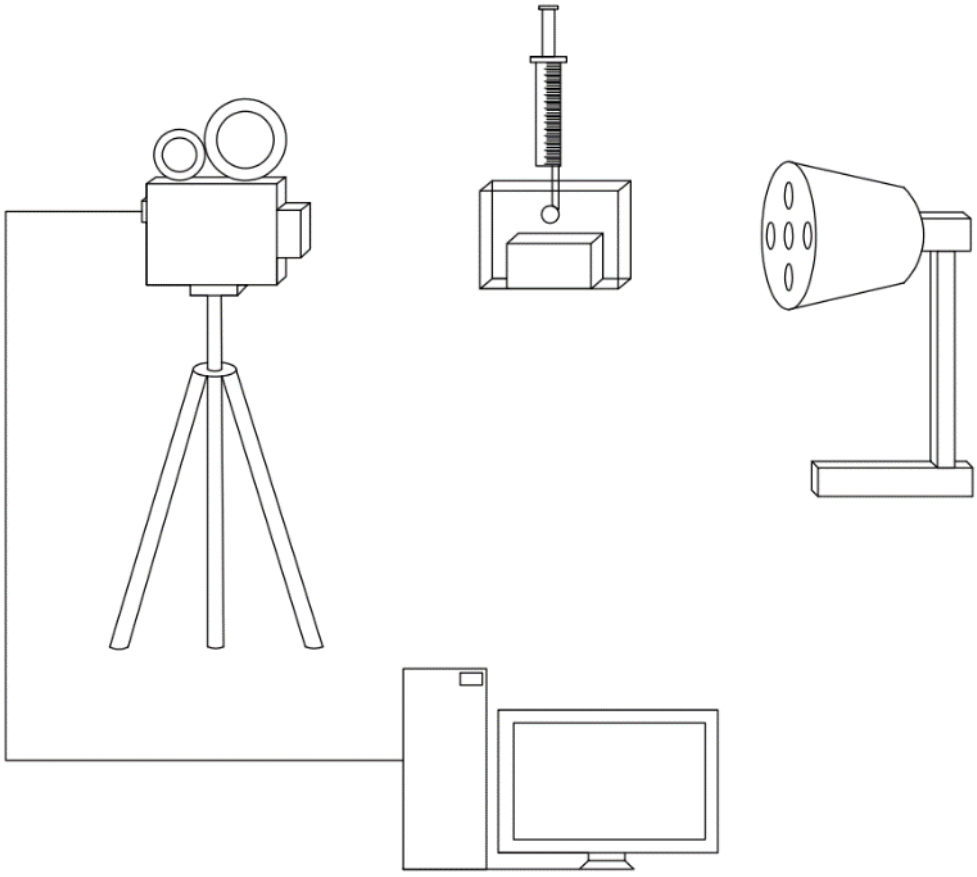

Figure 3. Schematic diagram of high-speed camera shooting.

The dynamic changes in the adhesion process of particles and bubbles can be effectively captured by a high-speed camera. The same shooting parameters such as magnification, exposure time, and number of recording frames have been adopted in similar

experiments. The experiment was repeated many times, and, finally, a representative result was obtained.

2.5. AFM Analysis

A Bruker Multimode 8 atomic force microscope (AFM, Bruker, Billerica, MA, USA) was used to study the surface topography of wolframite with or without nanobubbles and reagents. NanoScope Analysis software was used for data analysis and roughness calculation.

3. Results and Discussion

3.1. Bubble Size Distribution

In order to observe the size distribution of micro-nanobubbles, the clearer bubbles in the field of view were selected for measurement, and the results are shown in Figure 4.

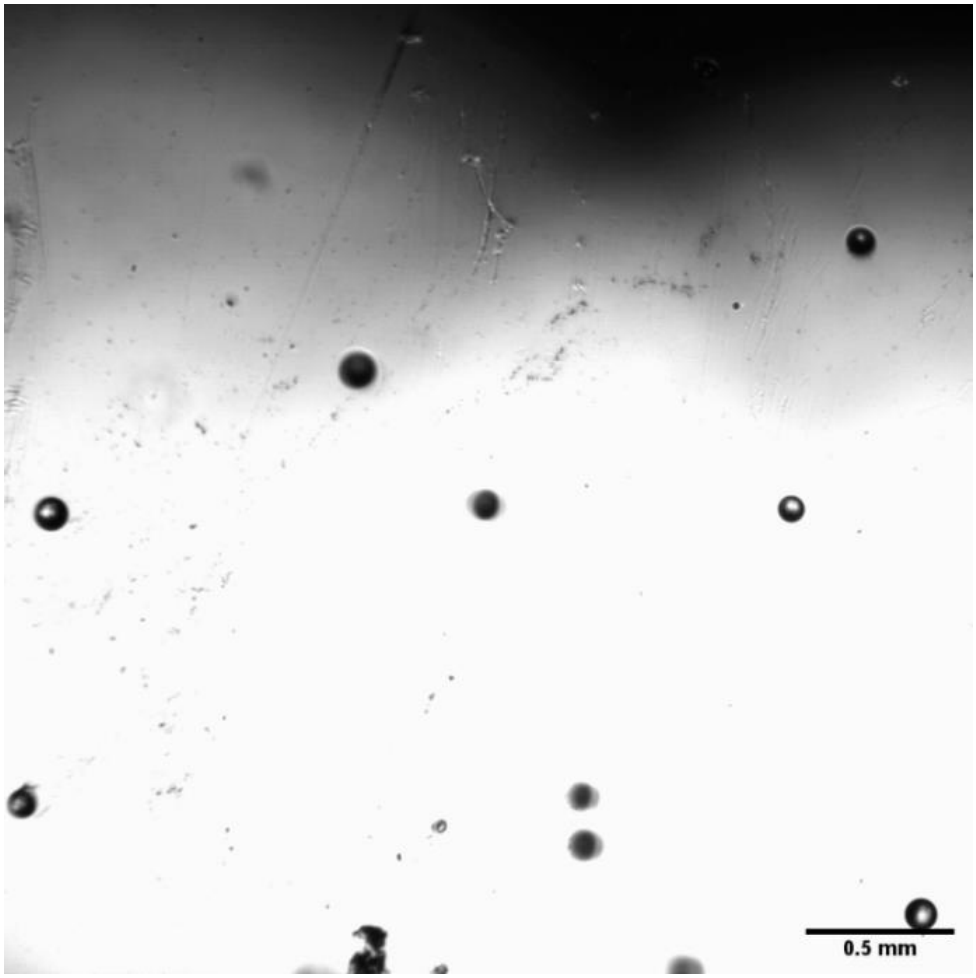

Figure 4. Representative bubbles.

As can be seen from Figures 4 and 5, the bubble size in the field of view is still between 70 and 120 μm, which belongs to the category of microbubbles. The foam stabilizer was not used here, the bubbles merge and burst spontaneously over time. This greatly affects the determination of bubble size and the measurement of gas holdup resulting in the nanobubbles disappearing quickly. Xu et al. [23] showed in their research that, due to the turbulent kinetic energy of the water flow that will hit the bubbles causing local loss of the water film of the microbubbles, this leads to an imbalance in the internal and external pressure of the microbubbles. Therefore, the microbubbles will merge and rupture in the

water, and during the flotation process, collisions will inevitably occur. This will also increase the instability of the microbubbles.

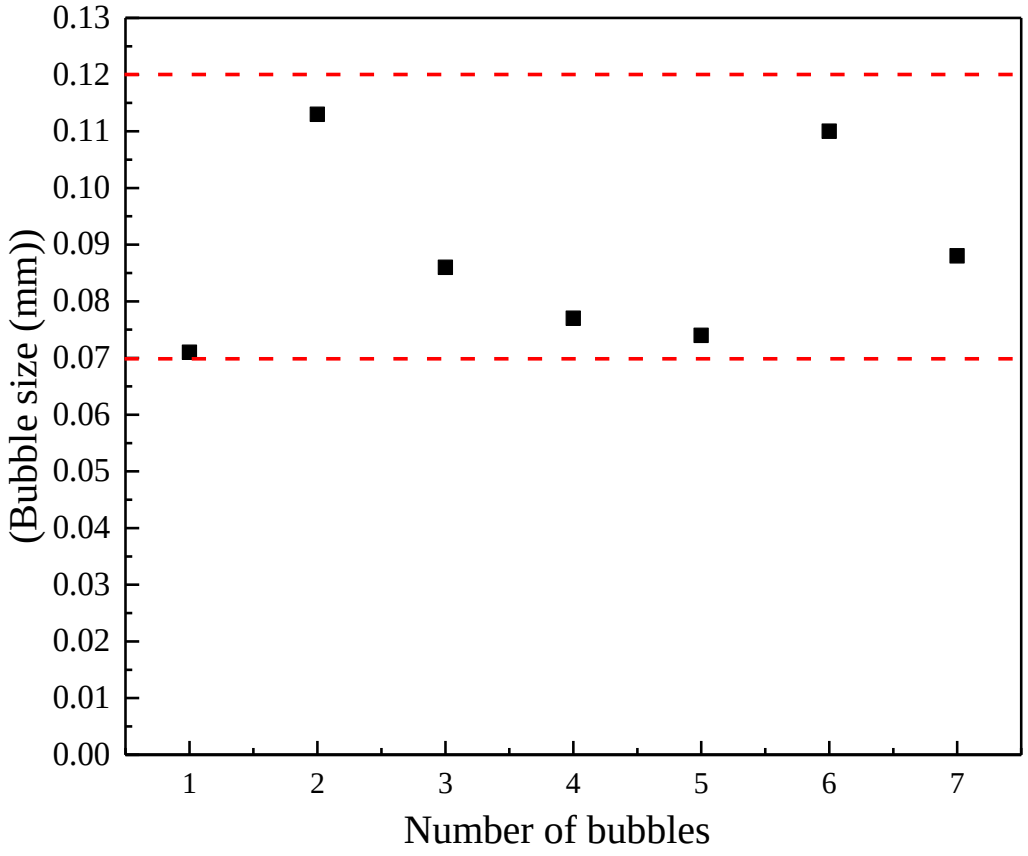

Figure 5. Bubble size distribution.

3.2. Effect of Micro-Nanobubbles on the Flotation of Fine Wolframite

A total of −20 μm fine-grain wolframite was used here. When pH is 10, the concentration of hydroxamic acid is 30, 50, 70, 90, 110, 130, 150 mg/L, respectively, the influence of micro-nanobubbles on the flotation of fine wolframite was investigated, and the results are shown in Figure 6.

As can be seen, the recovery significantly achieves an average increase of approximately 7% after being treated with microbubbles. The recovery of fine wolframite with or without microbubbles changed similarly with an increase in the concentration of hydroxamic acid. The recovery increases sharply with the increase in the concentration of hydroxamic acid. When the concentration of hydroxamic acid is 150 mg/L, the recovery of 85% can be obtained. In the same concentration of hydroxamic acid, the recovery of microbubble flotation of wolframite is about 15% higher than that of traditional flotation.

Rahman et al. [20] increased the recovery of fine chalcopyrite from 80% to 90% and ultrafine chalcopyrite from 55% to 75% by using nanobubbles. The results are compared with those of Ahmadi Rahman that showed that microbubbles are very suitable to be used in flotation with the brittle nature of minerals such as wolframite and chalcopyrite.

3.3. Effect of Microbubble on Zeta Potential

When pH is 3, 5, 7, 8, 9, 10, 11, 12, Zeta potential on the surface of wolframite measured was under the four conditions of pure water, octyl hydroxamic acid, micro-nanobubbles, and octyl hydroxamic acid plus micro-nanobubbles. The result is shown in Figure 7.

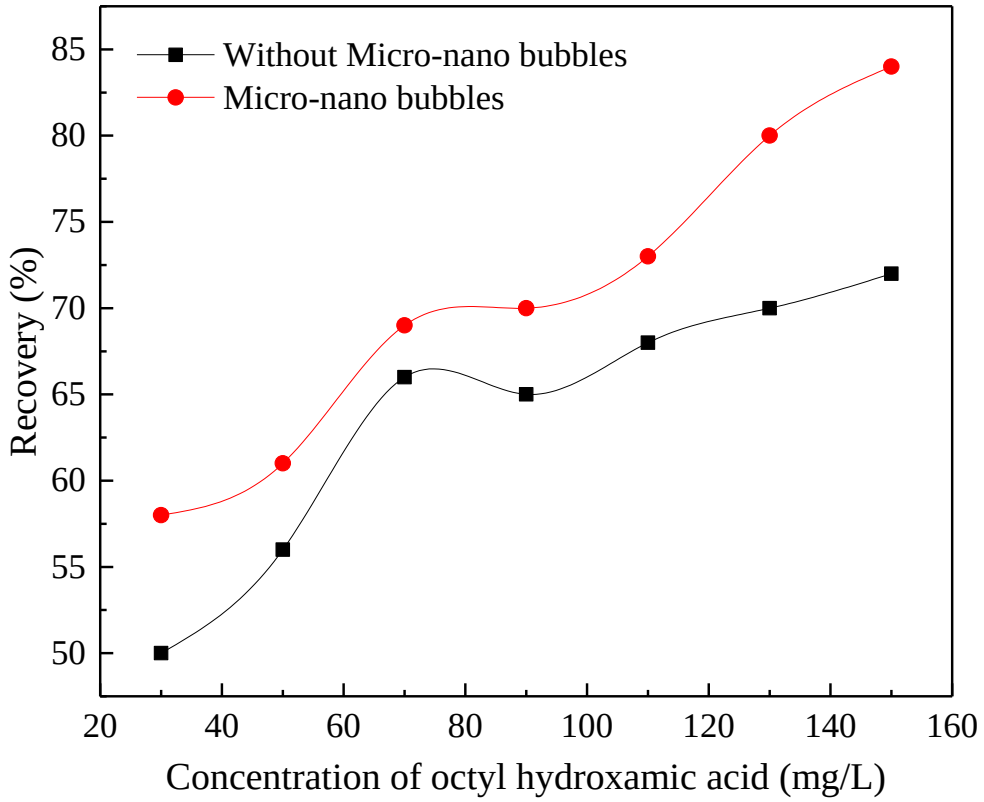

Figure 6. The relationship between the recovery rate and the amount of octyl hydroxamic acid (pH = 10).

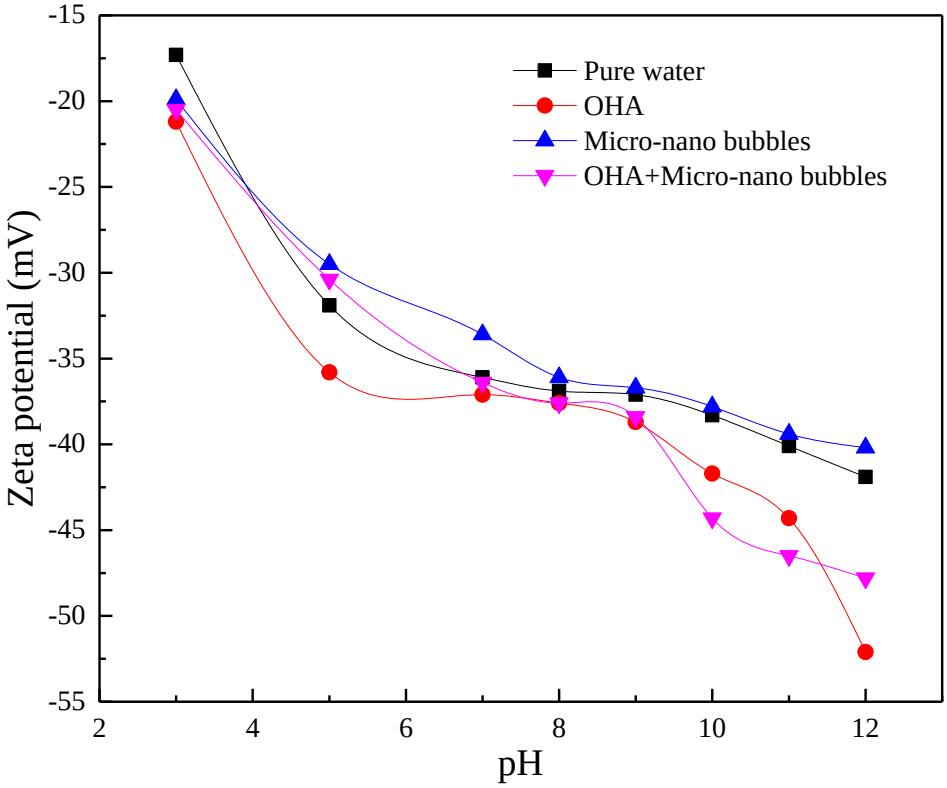

Figure 7. The relationship between the Zeta potential of wolframite and pH.

As shown in Figure 7, within the experimental range, a certain negative shift of the zeta potential on the wolframite surface with octyl hydroxamic acid is undergone. This shows that octyl hydroxamic acid is adsorbed on its surface. The zero point of wolframite is lower than 2. The wolframite has been agglomerated due to the microbubbles, and the zeta potential on the surface of the ore cluster is positively shifted. This facilitates the adsorption of negatively charged hydroxamic acid ions on its surface. This is also reflected in the maximum negative shift of zeta potential on the surface of wolframite with micro-nanobubbles and octyl hydroxamic acid in the vicinity of pH = 10 where the flotation recovery rate is the highest.

3.4. Interaction between Wolframite and Bubble

3.4.1. Agglomeration of Wolframite in Slurry under Different Conditions

A total of −20 μm fine-grain wolframite was used here. Equal amounts of pure water, micro-nanobubble aqueous solution, 70 mg/L octyl hydroxamic acid solution, and a mixed solution of microbubbles and 70 mg/L octyl hydroxamic acid were prepared as the solution to be observed. An equal amount of −20 μm wolframite was added into them and stirred to mix thoroughly. The image taken under the 4 × 10 times high-speed camera is shown in Figure 8.

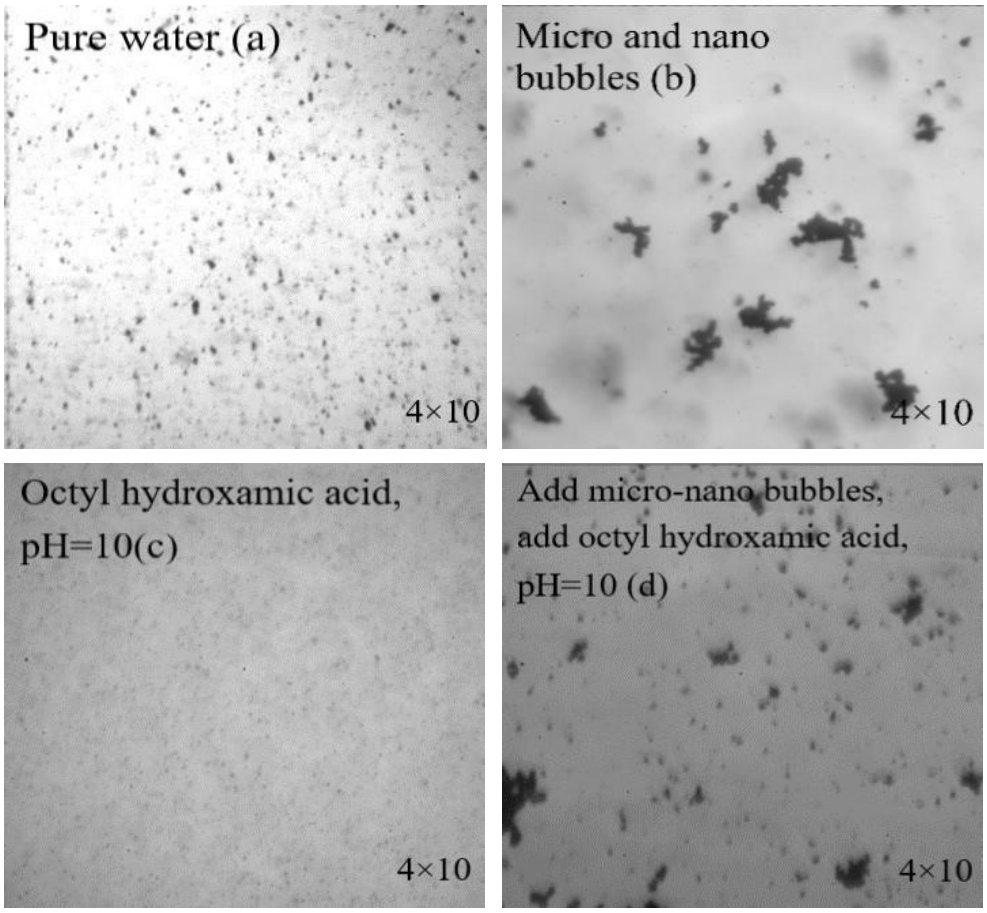

Figure 8. Agglomeration of ore particles under different conditions. (**a**) pure water, (**b**) micro and nano bubbles, (**c**) octyl hydroxamic acid, pH = 10, (**d**) add micro-nano bubbles and octyl hydroxamic acid, pH = 10.

Analyzing Figure 8 we can see that in the slurry solution (a,c), without adding micro-nanobubbles, the ore particles are evenly dispersed in the water. After adding the micro-nanobubbles (b,d), the mineral particles agglomerated obviously. This shows that micro-

nanobubbles can improve buoyancy by changing the agglomeration of mineral particles. Liu et al. [24] found through research that the trapping probability of bubbles is related to bubble size and particle size. In the case of a predetermined flotation mineral particle size, the probability of capture was greatly increased by reducing the bubble size. The longitudinal comparison of (a,b) and (c,d) in Figure 7 shows that the agglomeration form of the mineral particles in the slurry was not changed by the addition of the collector octyl hydroxamic acid. The study by Hu et al. [25] showed that with the increase in bubble size, the induction time gradually increased, which indicated that the adhesion of particles under the environment of small bubbles was good, and the mineralization performance of the bubble was also good.

3.4.2. Collision between Bubble and Mineral Particle

In total, −20 μm fine-grain wolframite was used to form an ore pile at the bottom of the observation vessel. The bubbles were blown by syringe air bubbles to make them float up after contact with the ore particles. A 4 × 1.62 × high-speed camera was used to observe the contact behavior of the bubbles and mineral particles, as shown in Figure 9.

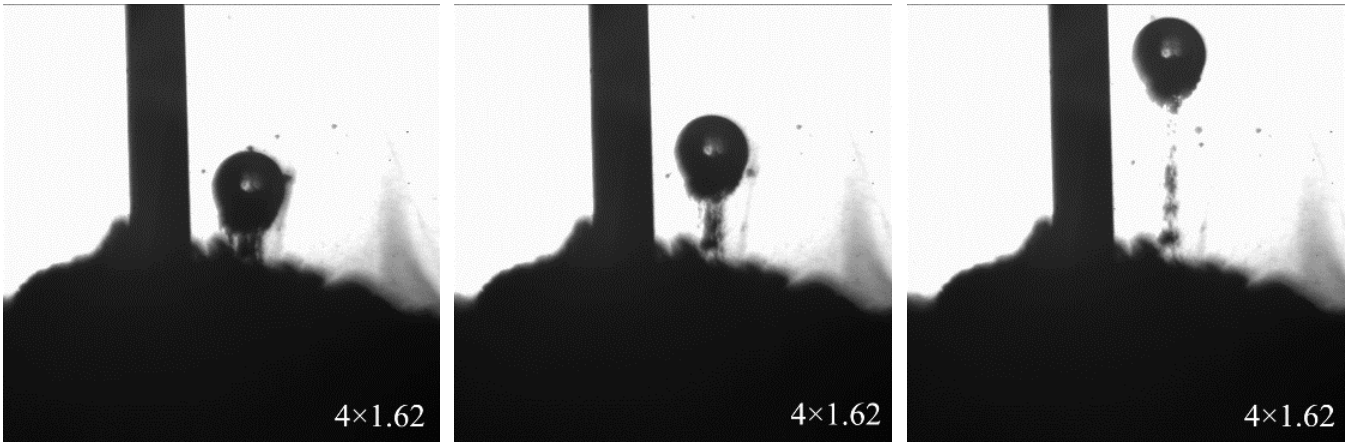

Figure 9. Contact of bubbles and mineral particles.

A relatively complete process of bubbles rising from the ore pile is shown in Figure 9. We can see that when the bubbles just rushed out of the ore pile, a large number of ore particles were carried on the surface of the bubbles. However, as the bubbles rise, more of the carried mineral particles gradually fall off. In the end, only a small amount of mineral particles remained at the bottom of the bubble and surfaced with the bubble. This shows that more mineral particles were not carried by a single large bubble, effectively using the bubble volume. The flotation efficiency will be affected during the flotation process.

3.4.3. Adhesion between Mineral Particles and Bubbles

The syringe was fixed in the observation dish in advance. The bubbles blown out of the syringe were kept within the field of view. A total of −20 μm fine wolframite was sprinkled from the top of the observation dish to the top of the bubbles leading the mineral particles and bubbles to actively make contact. A 10 × 1.43 times high-speed camera was used to observe the contact behavior of mineral particles and bubbles, as shown in Figure 10.

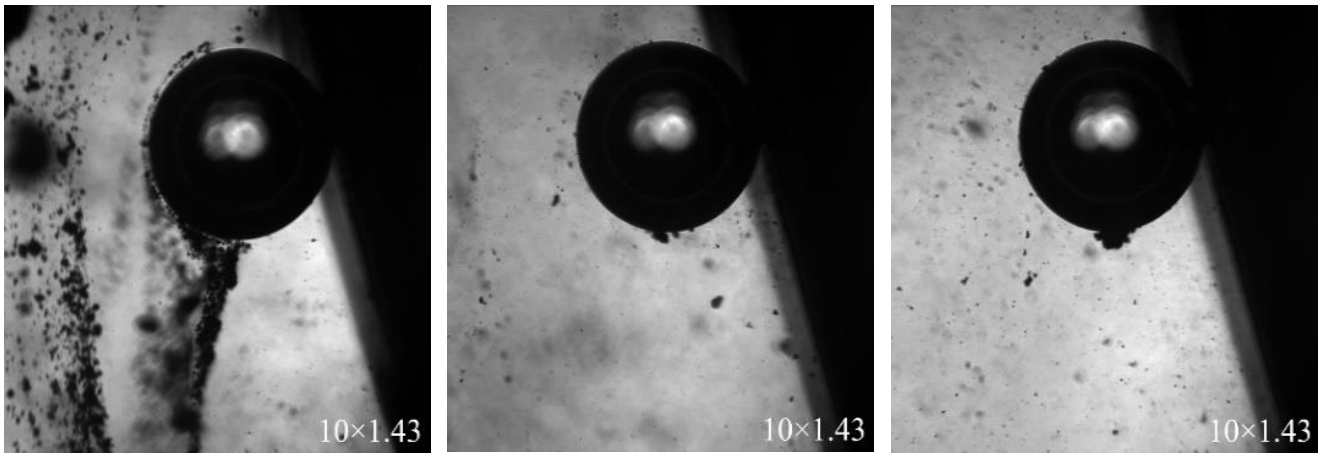

Figure 10. Contact between mineral particles and bubbles.

Figure 10 shows a relatively complete process of contact between mineral particles and air bubbles. When the mineral particles fall freely from above and contact the bubbles, the mineral particles will slide along the edge of the bubble to the bottom of the bubble and gradually gather together. At this time, the ore clusters will stick to the bottom of the bubbles and will not fall off. Zhang et al. [26] found that at this time, fine particles are more likely to move with the streamline and intercept and collide with bubbles.

According to the comparison between Figures 9 and 10, the collision behavior between mineral particles and bubbles mainly occurs at the bottom of the bubbles. When the ore particles accumulate to a certain amount at the bottom of the bubbles, the bubbles will not carry more ore particles to float up. The adhesion between the mineral particles and the bubbles is due to the squeezing of the hydration film between the bubbles and the particles gradually thinning until it ruptures, forming a stable three-phase contact line [27,28].

3.5. Effect of Microbubble on the Adsorption of OHA on the Wolframite Surface

In order to understand the adsorption state of octyl hydroxamic acid on the wolframite surface more intuitively, and to detect the coverage rate of the reagent and the thickness of the adsorption layer, the surface of the processed wolframite grinding disc was measured by AFM. The surface of the wolframite after the action of octyl hydroxamic acid was also observed. The two-dimensional and three-dimensional image results are shown in Figures 11 and 12. Among them, the side length of the scanning area is represented by the abscissa. The height of the highest point on the surface is represented by the ordinate. The scanning range is 10.0 μm × 10.0 μm and 3.0 μm × 3.0 μm, respectively. The greater the brightness in the image, the greater the height of the area. The height range of the surface of the clean wolframite grinding sheet is −93.6~546.4 nm. The height range of the wolframite surface after interaction with octyl hydroxamic acid is 207.6~454.1 nm.

Analyzing Figure 11 shows that the surface of clean wolframite is relatively smooth. From the 3D image on the right it can be seen that, although the height of the entire surface is quite different, the protrusions are not dense. There are fewer striped undulations on the surface that can eliminate the influence of the wolframite surface itself. A homogeneous and smooth wolframite surface was provided for testing. A sparse and uneven point-like adsorption morphology was shown on the wolframite surface from the heightmap in Figure 11, when octyl hydroxamic acid was not added. This shows that the wolframite has poor floatability.

The heightmap on the left side of Figure 12 shows that uneven plaques appear on the surface after the interaction of wolframite and octyl hydroxamic acid. It can be observed from the 3D picture on the right that the surface of the wolframite has changed significantly. There are a lot of peak-shaped protrusions, and the distribution is even and fine. This may

be due to the chemical bonding between octyl hydroxamic acid and the W atom on the wolframite surface, which is adsorbed on the wolframite surface.

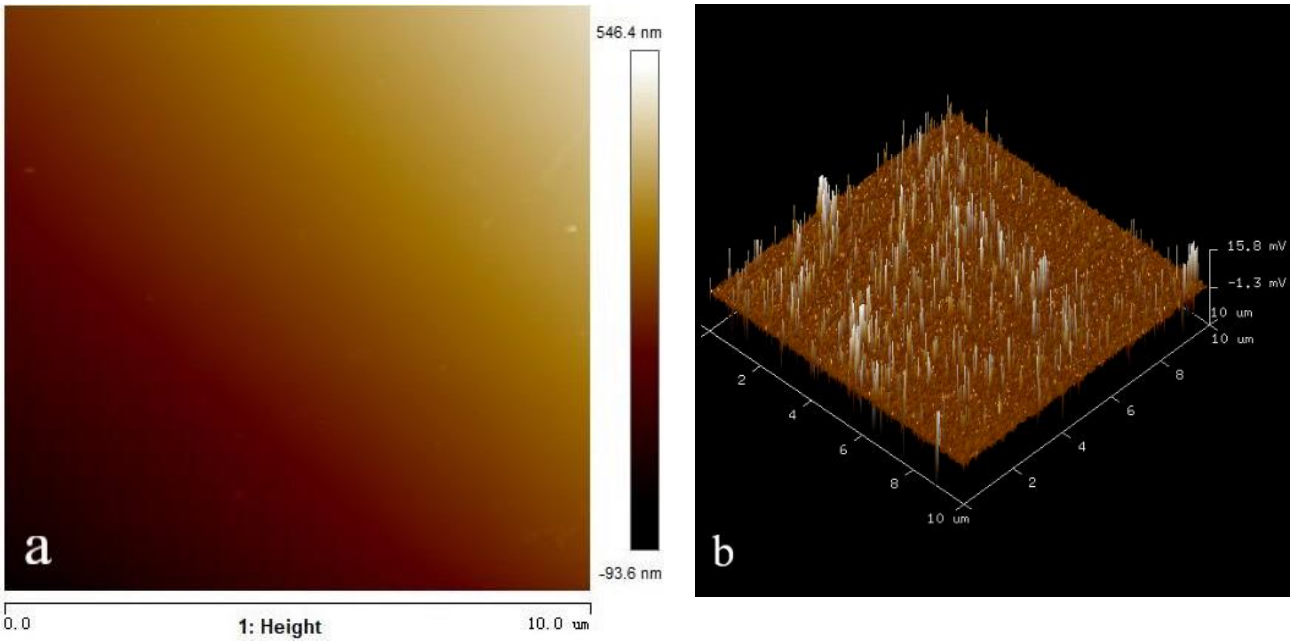

Figure 11. AFM morphology of wolframite grinding disc. (**a**) height (**b**) 3D.

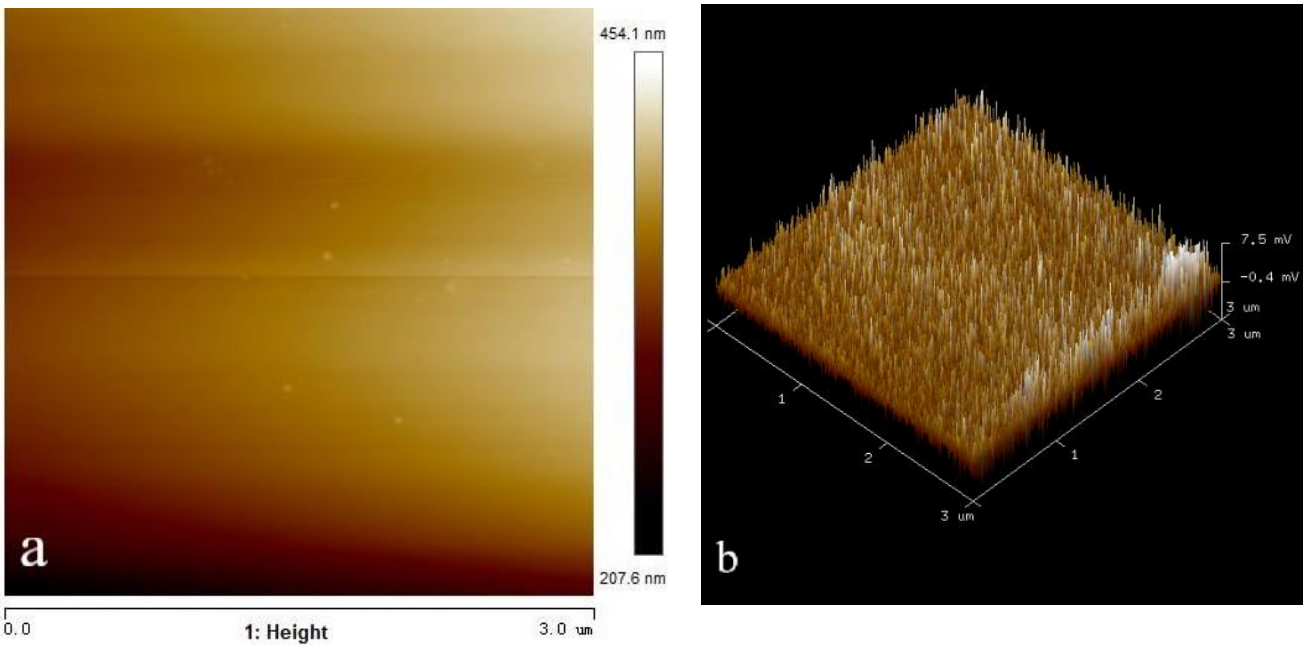

Figure 12. AFM morphology of wolframite grinding tablets after adding octyl hydroxamic acid (50 mg/L). (**a**) height (**b**) 3D.

Figure 13 shows that the spot adsorption on the wolframite surface is significantly reduced after adding octyl hydroxamic acid and micro-nanobubbles at the same time. The relative height of the suction protrusion is also reduced. The peak protrusions shown in the 3D image are no longer dense. This is because the microbubbles and the octyl hydroxamic acid produced competitive adsorption on the smooth wolframite surface. This replaces part of the role of collectors, thereby reducing the amount of collectors. The research of

Sabereh et al. [29] showed that nanobubbles will cover the hydrophobic surface of minerals, acting like a secondary collector for minerals.

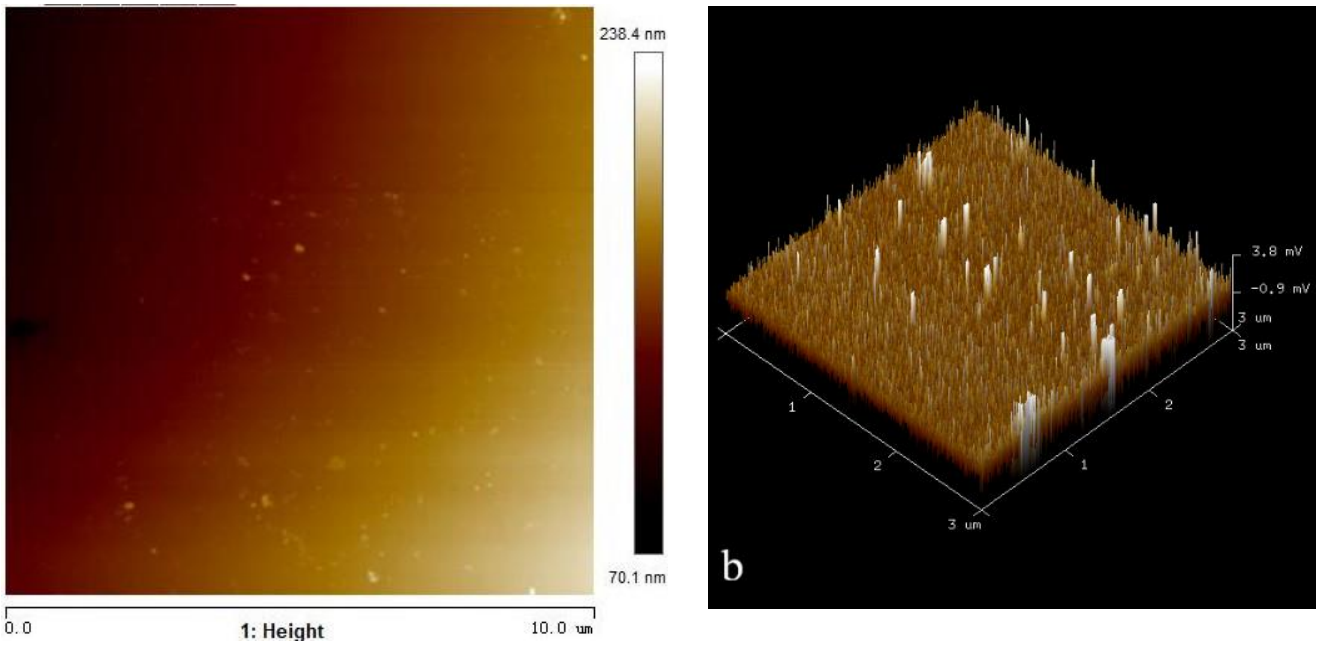

Figure 13. AFM morphology of wolframite grinding sheet after adding octyl hydroxamic acid (50 mg/L) and micro-nanobubbles. (**a**) height (**b**) 3D.

4. Conclusions

1. The introduction of micro-nanobubbles can significantly improve the recovery of fine wolframite flotation.
2. The fine-grain wolframite in the slurry had obvious agglomeration after adding microbubbles. The addition of microbubbles changed the agglomerating way of fine mineral particles, making it easier for fine wolframite particles to agglomerate together.
3. The AFM analysis results showed that the introduction of micro-nanobubbles on the surface of the flake wolframite reduced the adsorption of octyl hydroxamic acid, which resulted in the competitive adsorption of microbubbles and collectors.

Author Contributions: Conceptualization, P.W. and L.R.; methodology, P.W.; software, P.W.; validation, P.W., Y.Z. and L.R.; formal analysis, P.W.; investigation, P.W.; resources, S.B.; data curation, Y.Z.; writing—original draft preparation, P.W.; writing—review and editing, L.R.; visualization, S.B.; supervision, P.W.; project administration, Y.Z.; funding acquisition, S.B. All authors have read and agreed to the published version of the manuscript.

Funding: This research was funded by the National Natural Science Foundation of China, grant number U2003129, 51504175, Natural Science Foundation of Hubei Province, grant number 2019CFB533 and China Scholarship Council grant number 201706955031.

Conflicts of Interest: The authors declare no conflict of interest.

References

1. Gao, Y. The Characteristics and Research Advances of Mineral Processing Technologies of Chinese Tungsten Resources. *China Tungeten. Ind.* **2016**, *31*, 35–39. [CrossRef]
2. Ai, G.; Li, X. Study situation and prospects of concentration of micro-fine wolframite. *Min. Process. Equip.* **2011**, *39*, 89–96.
3. Farrokhpay, S.; Filippov, L.; Fornasiero, D. Flotation of Fine Particles: A Review. *Min. Proc. Ext. Met. Rev.* **2021**, *42*, 473–483. [CrossRef]

4. Zawala, J.; Karaguzel, C.; Wiertel, A.; Sahbaz, O.; Malysa, K. Kinetics of the bubble attachment and quartz flotation in mixed solutions of cationic and non-ionic surface-active substances. *Colloids Surf. A Physicochem. Eng. Asp.* **2017**, *523*, 118–126. [CrossRef]
5. Ai, G.; Yang, X.; Li, X. Flotation characteristics and flotation kinetics of fine wolframite. *Powder Technol.* **2017**, *305*, 377–381. [CrossRef]
6. Brabcová, Z.; Karapantsios, T.; Kostoglou, M.; Basařová, P.; Matis, K. Bubble–particle collision interaction in flotation systems. *Colloids Surf. A Physicochem. Eng. Asp.* **2015**, *473*, 95–103. [CrossRef]
7. Testa, F.G.; Safari, M.; Deglon, D.; Leal Filho, L.D.S. Influence of agitation intensity on flotation rate of apatite particles. *REM Int. Eng. J.* **2017**, *70*, 491–495. [CrossRef]
8. Li, M.; Xia, Y.; Zhang, Y.; Ding, S.; Rong, G.; Cao, Y.; Xing, Y.; Gui, X. Mechanism of shale oil as an effective collector for oxidized coal flotation: From bubble–particle attachment and detachment point of view. *Fuel* **2019**, *255*, 115885. [CrossRef]
9. Frederick Bloom, T.J.H. On the structure of collision and detachment frequencies in $otation models. *Chem. Eng. Sci.* **2002**, *57*, 2467–2473. [CrossRef]
10. Hassanzadeh, A.; Hassas, B.V.; Kouachi, S.; Brabcova, Z.; Çelik, M.S. Effect of bubble size and velocity on collision efficiency in chalcopyrite flotation. *Colloids Surf. A Physicochem. Eng. Asp.* **2016**, *498*, 258–267. [CrossRef]
11. Rulyov, N.N.; Filippov, L.O.; Kravchenko, O.V. Combined microflotation of glass beads. *Colloids Surf. A Physicochem. Eng. Asp.* **2020**, *598*, 124810. [CrossRef]
12. Fan, M.; Daniel, T.; Rick, H.; Luo, Z. Nanobubble generation and its application in froth flotation (part I): Nanobubble generation and its effects on properties of microbubble and millimeter scale bubble solutions. *Min. Sci. Technol.* **2010**, *20*, 1–19. [CrossRef]
13. Rh, Y. The role of hydrodynamic and surface forces in bubble–particle interaction. *Int. J. Miner. Process.* **2000**, *58*, 129–143. [CrossRef]
14. Safari, M.; Deglon, D. An attachment-detachment kinetic model for the effect of energy input on flotation. *Miner. Eng.* **2018**, *117*, 8–13. [CrossRef]
15. Safari, M.; Deglon, D. Evaluation of an Attachment–Detachment Kinetic Model for Flotation. *Minerals* **2020**, *10*, 978. [CrossRef]
16. Leila, Z.; Janet, A.W.E. Thermodynamics of Surface Nanobubbles. *Langmuir* **2016**, *32*, 11309–11320. [CrossRef]
17. Farrokhpay, S.; Filippova, I.; Filippov, L.; Picarra, A.; Rulyov, N.; Fornasiero, D. Flotation of fine particles in the presence of combined microbubbles and conventional bubbles. *Miner. Eng.* **2020**, *155*, 106439. [CrossRef]
18. Bu, X.; Zhang, T.; Chen, Y.; Xie, G.; Peng, Y. Comparative study of conventional cell and cyclonic microbubble flotation column for upgrading a difficult-to-float Chinese coking coal using statistical evaluation. *Int. J. Coal Prep. Util.* **2020**, *40*, 359–375. [CrossRef]
19. Santana, R.; Ribeiro, J.; Santos, M.; Reis, A.; Ataíde, C.; Barrozo, M. Flotation of fine apatitic ore using microbubbles. *Sep. Purif. Technol.* **2012**, *98*, 402–409. [CrossRef]
20. Ahmadi, R.; Khodadadi, D.A.; Abdollahy, M.; Fan, M. Nano-microbubble flotation of fine and ultrafine chalcopyrite particles. *Int. J. Min. Sci. Technol.* **2014**, *24*, 559–566. [CrossRef]
21. Rajeev, P.; Kumarmajumder, S.; Ghosh, P. Flotation of fine particles from binary mixture by ionic microbubbles. *ChemXpres* **2015**, *2*, 133–137.
22. Chen, B.; Bao, S.; Zhang, Y.; Zheng, R. Ultrasound-assisted synthesis of N235-impregnated resins for vanadium (V) adsorption. *R Soc. Open Sci.* **2018**, *5*, 171746. [CrossRef]
23. Xu, J. *Mechanism of Micro-bubble Air Flotation in Water Treatment Process. and Flotation Experiment*; Kunming University of Science and Technology: Kunming, China, 2013.
24. Liu, H.; Yang, C.; Wang, Y.; Gui, W. Influence analysis and parameter optimization of bubble diameter in Micro-bubbles flotation process. *Miner. Eng. Res.* **2009**, *24*, 58–61.
25. Hu, H.; Li, M.; Li, L.; Tao, X. Improving bubble-particle attachment during the flotation of low rank coal by surface modification. *Int. J. Min. Sci. Technol.* **2020**, *30*, 217–223. [CrossRef]
26. Zhang, S. *Study on Collision and Attachment Behavior Between Particle and Bubble in Coal Slime Flotation*; China University of Mining & Technology: Beijing, China, 2015.
27. Yang, J. *Visualized Study on the Interaction between Single Bubbles and Curved Solid Surface in Flotation Separation Process*; Chang'an University: Xi'an, China, 2014.
28. Ma, L. *Study on Minerals Particles Containing Calcium and Bubble Interaction*; Cental South University: Changsha, China, 2011.
29. Nazari, S.; Shafaei, S.; Gharabaghi, M.; Ahmadi, R.; Shahbazi, B.; Fan, M. Effects of nanobubble and hydrodynamic parameters on coarse quartz flotation. *Int. J. Min. Sci. Technol.* **2019**, *29*, 289–295. [CrossRef]